Estimation of main cable tension force of suspension bridges based on ambient vibration frequency measurements

Jun Wang[*], Weiqing Liu, Lu Wang and Xiaojian Han

College of Civil Engineering, Nanjing Tech University, Nanjing, China

Abstract.   In this paper, a new approach based on the continuum model is proposed to estimate the main cable tension force of suspension bridges from measured natural frequencies. This approach considered the vertical vibration of a main cable hinged at both towers and supported by an elastic girder and hangers along its entire length. The equation reflected the relationship between vibration frequency and horizontal tension force of a main cable was derived. To avoid to generate the additional cable tension force by sag-extensibility, the analytical solution of characteristic equation for anti-symmetrical vibration mode of the main cable was calculated. Then, the estimation of main cable tension force was carried out by anti-symmetric characteristic frequency vector. The errors of estimation due to characteristic frequency deviations were investigated through numerical analysis of the main cable of Taizhou Bridge. A field experiment was conducted to verify the proposed approach. Through measuring and analyzing the responses of a main cable of Taizhou Bridge under ambient excitation, the horizontal tension force of the main cable was identified from the first three odd frequencies. It is shown that the estimated results agree well with the designed values. The proposed approach can be used to conduct the long-term health monitoring of suspension bridges.

Keywords: tension force; main cable; suspension bridge; continuum model; anti-symmetrical vibration

1. Introduction

In the last few decades, suspension bridges have been employed increasingly in the civil engineering due to their advantages of long spans, low cost and high utilization of the materials. The main cables are a crucial element for overall structural safety of the bridge because most of the live and dead loads of suspension bridge are transferred to the anchorage systems by the main cables, hence, the accurate estimation of main cable tension force is essential for construction and maintenance inspection.

The current available techniques to estimate the cable tension force are the static methods and the vibration methods. For the static methods, the tension force can be directly measured by a load cell or a hydraulic jack, but they are too expensive and not suitable for maintenance stage. Recently, Yim *et al*. (2013) studied the effectiveness of elasto-magnetic (EM) sensors for monitoring the cable tension force. The results indicated that EM sensor can sensitively detect

---

∗Corresponding author, Associate Professor, E-mail: wangjun3312@njtech.edu.cn

average stress changes in cables. However, temperature effects on the relative permeability should be considered for accurate cable tension force measurement. While for the vibration methods, the tension force can be indirectly estimated from measured natural frequencies, thus the vibration methods are widely used because of its simplicity and convenience.

A number of experimental and theoretical studies have been conducted to estimate the cable tension force using vibration methods based on the taut string theory and the Bernoulli-Euler beam theory. Given the measured frequency and mode number, the cable tension force can be calculated straightforward based on the taut string theory. However, the application of this method which ignored the sag and flexural stiffness of the cables is strictly limited to a flat long slender cable (Casas 1994). The formulation from the Bernoulli-Euler beam theory considered the flexural stiffness, but it neglected the sag-extensibility. Fang and Wang (2012) proposed a practical formula in explicit expression to estimate cable force, and used the frequencies of the antisymmetric or higher modes of the cable to avoid the sag-extensibility effect. Other methods, with both flexural stiffness and sag-extensibility included, were also presented. Ricciardi and Saitta (2008) developed an analytical model for dynamics of large-diameter sagged cables by means of Hamilton's principle, but the proposed model had some limitations: (1) constant cable section; (2) no variation in boundary; (3) no external attachment; and (4) a sag-to-span ratio less than 1/8. Nam and Nghia (2011) studied the combined effects of flexural stiffness and sag-extensibility of the cable on its tension force. By introducing proper simplifying approximations, asymptotic forms for the wave number equation of an inclined cable considering flexural stiffness and sag-extensibility have been explicitly obtained. A set of practical formulas considering the effects of sag-extensibility and flexural stiffness have been proposed in which a prior knowledge of the axial and flexural stiffness of the cable is required (Zui *et al.* 1996, Yen *et al.* 1997, Mehrabi and Tabatabai 1998, Dan *et al.* 2014). However, the axial and flexural stiffness of an elastic cable were often unavailable or invalid in some practical cases (Kim *et al.* 2007).

For a suspender bridge, the dead loads of the girder and the distributed hangers are carried entirely by the main cable, and the vibration of a main cable is influenced by the effects of hangers and stiffening girder. The study of the dynamic behavior of suspender bridges including the stiffening girder has been initiated since the collapse of Tacoma Narrows Bridge in 1940. The earlier study results presented that the effects of shear deformation and rotary inertia of the stiffening girder were relatively small and only affected the higher modes of vibration (Kim *et al.* 2000). In addition, McKenna and Walter (1987) and others (Lazer and McKenna 1990, Glover *et al.* 1989, Holubova-Tajcova 1999, McKenna and Moore 2002, Humphreys and McKenna 2005) presented a series of papers to explore the possibility of nonlinear oscillations of suspension bridges arising from the slackening of the hangers. Recently, Turmo and Luco (2010) studied the effect of flexibility of the hangers on vertical vibrations of suspension bridges. They found that the effect become more significant for the higher modes, particularly for stiff girders. Konstantakopoulos and Michaltsos (2010) proposed a mathematical model for the combined cable system of bridges. The model ignored the influence of bridge girder roughness and replaced the influence of hangers and stays with distributed loads. Luco and Turmo (2010) extended the analytical and numerical results of natural frequencies, mode shapes and modal participation factors for an extensible suspension cable to the case of a stiffened suspension bridge.

Recently, many studies have been conducted to estimate the cable tension force with finite element (FE) method. Ni *et al.* (2002), Kim and Park (2007) established a FE model which considered both sag-extensibility and flexural stiffness for a target cable system to identify the model using frequency-based sensitivity- updating algorithm. Wang *et al.* (2010) developed a

baseline model for the Runyang Suspension Bridge, then used it for the continuous structural health monitoring of the bridge. Brownjohn *et al.* (2001) studied the sensitivity analysis based on FE model updating method and used it to assess the structural behavior with particular reference to bridges. The results demonstrated that the accurancy of model updating method was affected by the number of measurements. Schlune *et al.* (2009) proposed a methodology to eliminate inaccurate modeling simplification by means of manual model refinements before parameters were estimated by non-linear optimization. Liao *et al.* (2012) formulated a precise FE model accounting for cable flexural stiffness, sag-extensibility, spatial variability of dynamic tension, boundary conditions, lumped masses and intermediate supports and/or dampers as the reference model in parameter identification, so that the modeling error was minimized. Although FE model updating method can be applied to a wide range of cable structures, more generic studies are best undertaken by use of continuum models. Simple continuum formulations can directly describe a general cable structure with a minimum number of parameters.

Although the studies on vibration methods are extensive, there are no suitable vibration methods to directly measure the tension force of main cable in maintenance stage. Moreover, the existing vibration methods to estimate the tension forces of hangers and stayed-cables from measured natural frequencies are not suitable to estimate the tension forces of main cables of suspension bridge, because the vibration of a main cable is influenced by the hangers and stiffening girder. Hence, estimating the tension force of a main cable in maintenance stage has not been solved.

To address the aforementioned shortcomings, a simple and innovative continuum model is proposed to estimate the main cable tension force of suspension bridges from measured frequencies. In this model, the elastic stiffening main cable, elastic stiffening girder and distributed elastic hangers with spatially variable stiffnesses are considered. The main cable is simplified as a one-dimensional structure hinged at both towers and flexural stiffness is added as a beam-like structure. Meanwhile, the girder and hangers provide additional elastic supports for the main cable along its entire length. Then, the differential equation of motion governing the vertical vibration of a main cable is obtained by introducing translational spring constant term associated with the girder and hangers, and the characteristic frequency formula of a main cable is utilized to estimate the main cable tension force. An application on a main cable of Taizhou Bridge is conducted to validate this new model.

2. Free vertical vibration of the main cable model

In this model, we assume that the main cables are hinged at the towers and supported by an elastic girder and distributed hangers along its entire length; the shear deformation and the rotator inertia of the main cable are ignored; the hangers are considered to be non-mass and elasticity, and the initial uniform dead load on the girder is carried by the main cable without causing any stress in the stiffening girder. Hence the main cable can be described by a parabolic profile under the initial dead load. The forces on a main cable segment with the length of *dx* are shown in Fig. 1.

The equation of free vibration for the main cable is given as

$$E_c I_c \frac{\partial^4 w}{\partial x^4} - H_w \frac{\partial^2 w}{\partial x^2} - h(t)\frac{\partial^2 z}{\partial x^2} + m\frac{\partial^2 w}{\partial t^2} + \sum_{i=1}^{N} k_i w(x_i, t)\delta(x - x_i) = 0 \qquad (1)$$
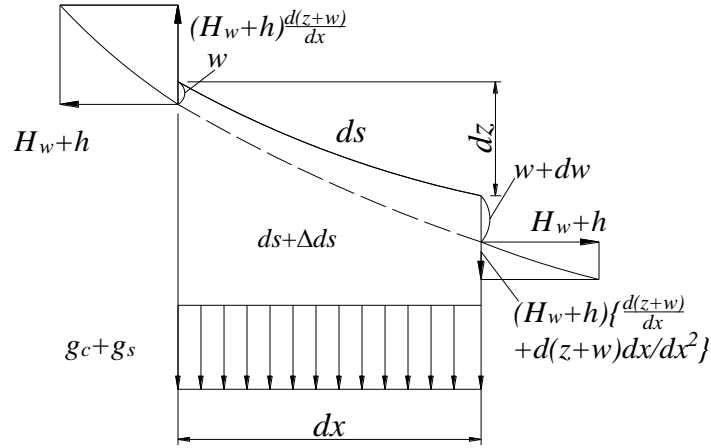
Fig. 1 Equilibrium of an infinitesimal part of a main cable

where w is the vertical displacement of the main cable, m is the combined mass of a main cable and the girder per unit length along the main cable, E_cI_c is the effective flexural stiffness of the main cable, H_w is the horizontal component of main cable tension force under dead load, $h(t)$ is the horizontal component of the increment of main cable tension force, $z(x)$ is the parabolic profile of the main cable under dead load, N is the number of hangers, k_i is the equivalent stiffness of the ith hangers and the girder, and $\delta(x-x_i)$ is the Dirac delta function.

The function $h(t)$ can be calculated by Eq. (2) (Timoshenko and Young 1965).

$$h(t) = \frac{8E_cA_cf}{L_eL^2} \int_0^L w(x,t)dx \tag{2}$$

where E_c is the Young modulus of the main cable, A_c is the cross sectional area of the main cable, f is the maximum (centre) sag of the main cable, and L is the main span of suspension bridges.

The length L_e can be expressed as

$$L_e = \int_0^L \left(\frac{ds}{dx}\right)^3 dx = \int_0^L \left[1+\left(\frac{dz}{dx}\right)^2\right]^{3/2} dx \approx L\left[1+8\left(\frac{f}{L}\right)^2\right] \tag{3}$$

In the case of anti-symmetric vibration, $\int_0^L w(x,t)dx = 0$ and the mode shape is given by

$$\phi_n(x) = sin\left(\frac{n\pi x}{L}\right) \tag{4}$$

Thus the equation for the anti-symmetric free vibration of the main cable is

$$E_cI_c\frac{\partial^4 w}{\partial x^4} - H_w\frac{\partial^2 w}{\partial x^2} + m\frac{\partial^2 w}{\partial t^2} + \sum_{i=1}^N k_i w(x_i,t)\delta(x-x_i) = 0 \tag{5}$$

According to the mode superposition theory, the vertical displacement of anti-symmetric vibration of the main cable can be assumed to take the form

$$w(x,t) = \sum_{n=1}^{\infty} \varphi_{2n}(x) Z_{2n}(t) \tag{6}$$

where $\varphi_{2n}(x)$ is the $2n$ th "normal" mode shape of the main cable, and $Z_{2n}(t)$ is the associated $2n$ th generalized coordinate.

If the axial stiffness of hangers is infinite, then the equivalent stiffness of the girder with respect to the main cable k_i' is determined by the flexural stiffness of girder. Using the orthogonal property of the mode shapes

$$\int_0^L \frac{k_i'}{L/N} \varphi_{2n}^2(x) dx = \int_0^L E_b I_b \frac{d^4 \varphi_{2n}(x)}{dx^4} \varphi_{2n}(x) dx \tag{7}$$

where N is the number of hangers, and $E_b I_b$ is the flexural stiffness of the girder.

From Eq. (7), k_i' is given by

$$k_i' = \left[\frac{2n\pi}{L} \right]^4 \frac{E_b I_b L}{N} \tag{8}$$

Connecting the axial stiffness of hangers in series with the flexural stiffness of girder will lead to the equivalent stiffness k_i in the form

$$k_i = \left[k_i' \frac{E_s A_s}{l_i} \right] \Big/ \left[k_i' + \frac{E_s A_s}{l_i} \right] \tag{9}$$

where E_s, A_s and l_i are the Young's modulus, cross-sectional area and length of the ith hangers, respectively.

Substituting Eq. (6) into Eq. (5), and multiplying $\phi_s(x)$ to both side of Eq. (1), then integrating each term over the main span L

$$m \sum_{n,s=1}^{\infty} \int_0^L \varphi_{2n}(x) \varphi_{2s}(x) dx \ddot{Z}_{2n}(t) + E_c I_c \sum_{n,s=1}^{\infty} \int_0^L \frac{d^4 \varphi_{2n}(x)}{dx^4} \varphi_{2s}(x) dx Z_{2n}(t)$$

$$-H_w \sum_{n,s=1}^{\infty} \int_0^L \frac{d^2 \varphi_{2n}(x)}{dx^2} \varphi_{2s}(x) dx Z_{2n}(t) + \int_0^L \sum_{i=1}^{N} k_i \left[\sum_{n,s=1}^{\infty} \varphi_{2n}(x_i) Z_{2n}(t) \right] \delta(x - x_i) \varphi_{2s}(x) dx = 0 \tag{10}$$

According to the orthogonal property of the mode shapes, Eq. (10) can be expressed as

$$M \ddot{Z}_{2n}(t) + \left(K_C - K_H + K_S \right) Z_{2n}(t) = 0 \tag{11}$$

where M is related to the mass introduced by the main cable and girder, K_C, K_H, and K_S are related to the stiffness introduced by the elasticity of the main cable, the static tension H_w and the equivalent stiffness of the hangers and a girder. Full expressions for the above coefficients are

$$M = m \int_0^L \varphi_{2n}^2(x) dx \tag{12}$$

$$K_C = E_c I_c \int_0^L \varphi_{2n}'''(x) \varphi_{2n}(x) dx \tag{13}$$

$$K_H = H_w \int_0^L \varphi_{2n}''(x) \varphi_{2n}(x) dx \tag{14}$$

$$K_S = \sum_{i=1}^N k_i \varphi_{2n}^2(x_i) \tag{15}$$

In the case of anti-symmetric vibrations, the mode shape is given by Luco and Turmo (2010)

$$\varphi_{2n}(x) = C_{2n} \sin\left(\frac{2n\pi x}{L}\right) \tag{16}$$

Putting Eq. (16) into Eqs. (12)-(15) gives

$$M = \frac{mL}{2} \tag{17}$$

$$K_C = \left(\frac{2n\pi}{L}\right)^4 \frac{E_c I_c L}{2} \tag{18}$$

$$K_H = \left(\frac{2n\pi}{L}\right)^2 \frac{H_w L}{2} \tag{19}$$

$$K_S = \sum_{i=1}^N k_i \sin^2\left(\frac{2n\pi x_i}{L}\right) \tag{20}$$

Substituting Eqs. (17) - (20) in Eq. (11), the $2n$ *th* anti-symmetric characteristic frequency ω_{2n} is given by

$$\left(\frac{2n\pi}{L}\right)^4 \frac{E_c I_c L}{2} + \left(\frac{2n\pi}{L}\right)^2 \frac{H_w L}{2} - \omega_{2n}^2 \frac{mL}{2} = -\sum_{i=1}^N k_i \sin^2\left(\frac{2n\pi x_i}{L}\right) \tag{21}$$

3. Parametric variation of characteristic frequencies

It is convenient to introduce dimensionless formulation to elucidate the effect of parametric variation on characteristic frequencies. As mentioned by Luco and Turmo (2010), the dimensionless $\bar{x}$, $\bar{t}$ and $\bar{w}$ were used to replace the variables, in which $\bar{x} = x/L$, $\bar{t} = t\sqrt{g/8f} = \frac{t}{L}\sqrt{H/m}$ and $\bar{w}(\bar{x}, \bar{t}) = w(x,t)/8f$. Thus, Eq. (1) can be transferred to the dimensionless equation of vibration

$$\mu_c^2 \frac{\partial^4 \bar{w}}{\partial \bar{x}^4} - \frac{\partial^2 \bar{w}}{\partial \bar{x}^2} + \lambda^2 \int_0^1 \bar{w} d\bar{x} + \sum_i^N \bar{k}_i \bar{w}(\bar{x}, \bar{t}) \delta(\bar{x} - \bar{x}_i) = 0 \tag{22}$$

where

$$\mu_c^2 = E_c I_c / H L^2 \tag{23}$$

$$\lambda^2 = \left(\frac{8f}{L}\right)^2 \left(\frac{L}{L_e}\right)\left(\frac{E_c A_c}{H}\right) \tag{24}$$

and

$$\overline{k}_i = k_i \frac{8f}{mgL} \tag{25}$$

For anti-symmetric vibration, the dimensionless equation of free vibration is given by

$$\mu_c^2 \frac{\partial^4 \overline{w}}{\partial \overline{x}^4} - \frac{\partial^2 \overline{w}}{\partial \overline{x}^2} + \sum_i^N \overline{k}_i \overline{w}(\overline{x},\overline{t})\delta(\overline{x} - \overline{x}_i) = 0 \tag{26}$$

Substituting the dimensionless into Eq. (21), the natural anti-symmetric frequencies $\overline{\omega}_{2n}$ is given by

$$\frac{\mu_c^2 (2n\pi)^4}{2} + \frac{(2n\pi)^2}{2} - \frac{\overline{\omega}_{2n}^2}{2} = -\sum_{i=1}^N \overline{k}_i \sin^2\left(2n\pi\overline{x}_i\right) \tag{27}$$

where

$$\overline{\omega}_{2n} = \omega_{2n}\sqrt{\frac{8f}{g}} \tag{28}$$

The parameter μ_c^2 reflects the relative flexural stiffness of the main cable (Luco and Turmo (2010) and Steinman (1953)). The Irvine-Caughey cable parameter λ^2 accounts for the relationship between the elastic and geometric stiffnesses of the main cable (Irvine and Caughey (1974)).

If all the hangers are perfectly flexible ($\frac{E_s A_s}{l_i} = 0$), then $\overline{k}_i = 0$.

If all the hangers are inextensible, then $\overline{k}_i$ is determined by the flexural stiffness of the girder

$$\overline{k}_i = k_i' \frac{8f}{mgL} = (2n\pi)^4 \frac{\mu_b^2}{N} \tag{29}$$

where

$$\mu_b^2 = E_b I_b / HL^2 \tag{30}$$

Figs. 2(a) to (c) show the first three anti-symmetric natural frequencies varied with different values of μ_b^2 and μ_c^2 for $N=50$ in the cases of inextensible and perfectly flexible hangers, respectively. It is indicated that the first three anti-symmetric frequencies are relatively independent of μ_c^2 for the value of $\mu_c^2 < 0.0025$, which is consistent with the results presented in Luco and Turmo (2010). For $\mu_c^2 > 0.0025$, the effects of μ_c^2 on the anti-symmetric frequencies appear to increase with the decreasing of μ_b^2. Moreover, the anti-symmetric frequencies for $\overline{k}_i = 0$ and $\mu_b^2 = 0.001$ are almost identical. To study the effect of N on natural frequencies, Table 1 shows numerical values for the first anti-symmetric natural frequencies with $N=50$ and
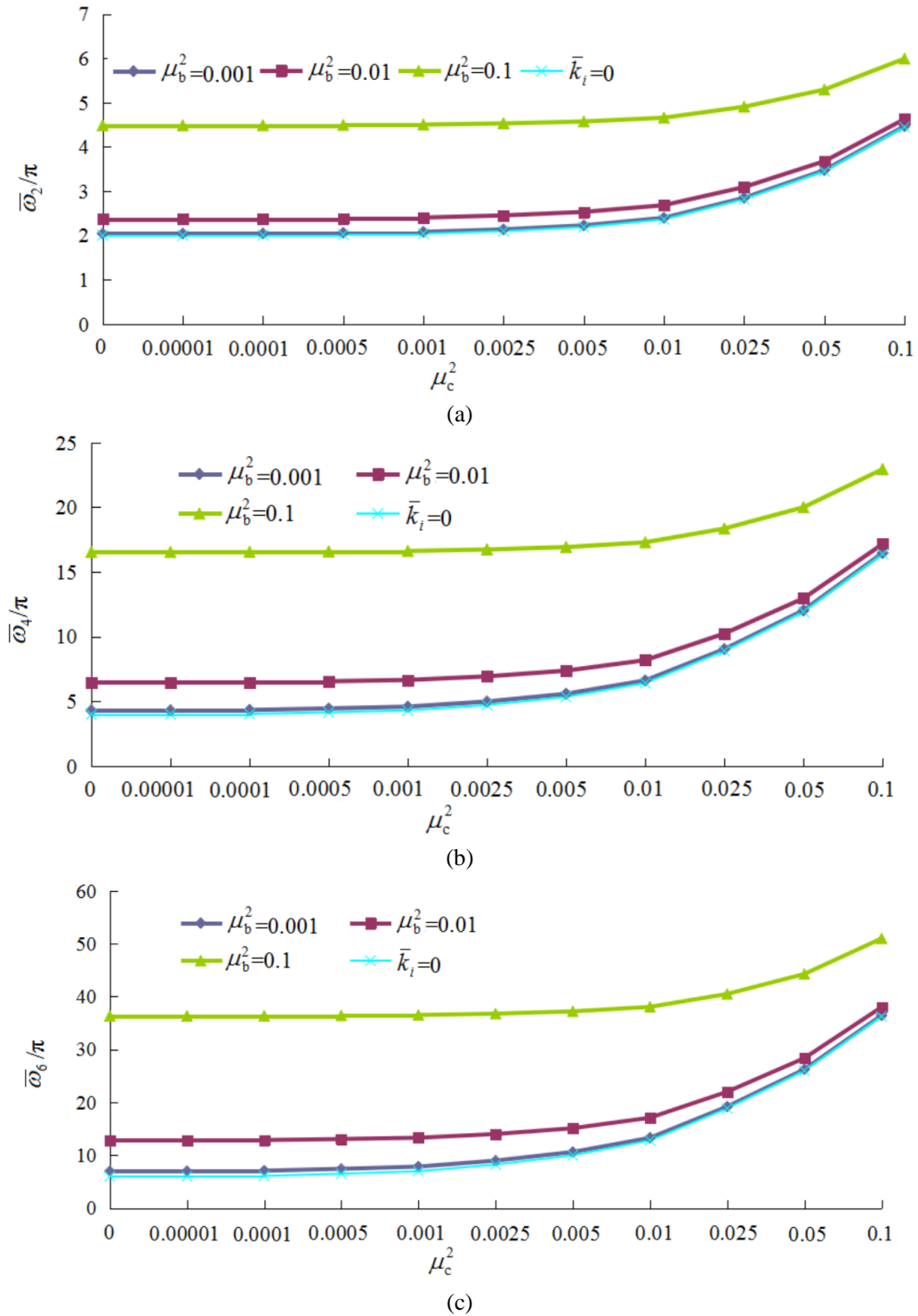
(a)

(b)

(c)

Fig. 2 Effects of μ_c^2, μ_b^2 and $\bar{k}_i = 0$ on the natural frequencies of the first three anti-symmetric modes: (a) $\bar{\omega}_2/\pi$, (b) $\bar{\omega}_4/\pi$, and (c) $\bar{\omega}_6/\pi$

Table 1 The first anti-symmetric natural frequencies $\bar{\omega}/\pi$ for N=50 and N=100

μ_c^2	$\mu_b^2 = 0.001$		$\mu_b^2 = 0.01$		$\mu_b^2 = 0.1$	
	N=50	N=100	N=50	N=100	N=50	N=100
0	2.040	2.040	2.369	2.365	4.483	4.466
0.00001	2.040	2.040	2.369	2.366	4.483	4.466
0.0001	2.044	2.043	2.372	2.369	4.485	4.467
0.0005	2.059	2.059	2.385	2.382	4.492	4.474
0.001	2.078	2.078	2.402	2.398	4.501	4.483
0.0025	2.134	2.134	2.450	2.447	4.527	4.510
0.005	2.225	2.224	2.530	2.526	4.570	4.553
0.01	2.396	2.395	2.681	2.678	4.656	4.639
0.025	2.847	2.847	3.090	3.088	4.903	4.887
0.05	3.471	3.471	3.674	3.672	5.290	5.275
0.1	4.465	4.465	4.624	4.623	5.990	5.976

N=100, respectively. It is found that the number of hangers has an insignificant effect on the first anti-symmetric natural frequencies.

4. Estimation of main cable tension force

Given the measured anti-symmetric characteristic frequencies, this paper deals with the problems how to identify the horizontal tension force, flexural stiffness of a main cable, as well as the combined mass of the main cable and girder per unit length along the main cable. Estimating the tension forces of main cables in suspension bridges is essential for regular inspection and health assessment of those structures. The horizontal tension force is selected for an identification variable because it is a constant. In addition, the reason why to select the flexural stiffness of a main cable and the combined mass of main cable and girder per unit length along the main cable is that such material properties are associated with the health condition of a bridge, and usually unavailable in some practical cases. In order to avoid the influence of $h(t)$, the anti-symmetric characteristic frequencies are adopted to estimate H_w, E_cI_c and m. From Eq. (21), the anti-symmetric characteristic frequency function can be written as

$$Z_{2n \times 1} = X_{2n \times 3} \lambda_{3 \times 1} \tag{31}$$

where

$$Z = \begin{bmatrix} -K_{2S} & -K_{4S} & \cdots & -K_{2nS} \end{bmatrix}^T \tag{32}$$

$$X = \begin{bmatrix} 2^4 \left(\dfrac{\pi}{L}\right)^2 \dfrac{L}{2} & \left(\dfrac{\pi}{L}\right)^2 \dfrac{L}{2} & -\dfrac{\omega_2^2}{2} \\ 4^4 \left(\dfrac{\pi}{L}\right)^2 \dfrac{L}{2} & \left(\dfrac{4\pi}{L}\right)^2 \dfrac{L}{2} & -\dfrac{\omega_4^2}{2} \\ \cdots & \cdots & \cdots \\ (2n)^4 \left(\dfrac{\pi}{L}\right)^2 \dfrac{L}{2} & \left(\dfrac{2n\pi}{L}\right)^2 \dfrac{L}{2} & -\dfrac{\omega_{2n}^2}{2} \end{bmatrix} \tag{33}$$

$$\lambda = \left[\frac{\pi^2 E_c I_c}{L^2} \quad H_w \quad ml \right]^T \tag{34}$$

The presence of inevitable measurement noise introduces unequal on both sides of the Eq. (31). Considering the error ε between Z and $\tilde{Z}$,

$$\tilde{Z} = \tilde{X}\tilde{\lambda} + \varepsilon \tag{35}$$

where the symbol '~' indicates approximate values.

$$\tilde{Z} = \left[-\tilde{K}_{2S} \quad -\tilde{K}_{4S} \quad \cdots \quad -\tilde{K}_{2nS} \right] \tag{36}$$

$$\tilde{X} = \begin{bmatrix} 2^4 \left(\frac{\pi}{L}\right)^2 \frac{L}{2} & \left(\frac{2\pi}{L}\right)^2 \frac{L}{2} & -\frac{\tilde{\omega}_2^2}{2} \\ 4^4 \left(\frac{\pi}{L}\right)^2 \frac{L}{2} & \left(\frac{4\pi}{L}\right)^2 \frac{L}{2} & -\frac{\tilde{\omega}_4^2}{2} \\ \cdots & \cdots & \cdots \\ (2n)^4 \left(\frac{\pi}{L}\right)^2 \frac{L}{2} & \left[\frac{2n\pi}{L}\right]^2 \frac{L}{2} & -\frac{\tilde{\omega}_{2n}^2}{2} \end{bmatrix} \tag{37}$$

$$\tilde{\lambda} = \left[\frac{\pi^2 \tilde{E}_c \tilde{I}_c}{L^2} \quad \tilde{H}_w \quad \tilde{m}L \right]^T \tag{38}$$

$$\varepsilon = \left[\varepsilon(2) \quad \varepsilon(4) \quad \cdots \quad \varepsilon(2n) \right]^T \tag{39}$$

From Eq. (35), error vector can be calculated by

$$\varepsilon = \tilde{Z} - \tilde{X}\lambda \tag{40}$$

Based on the principle of least-squares, $\tilde{\lambda}$ can be estimated by the following equation

$$\tilde{\lambda} = \left(\tilde{X}^T \tilde{X} \right)^{-1} \tilde{X}^T \tilde{Z} \tag{41}$$

Therefore, parameters of H_w, $E_c I_c$ and m can be extracted from vector $\tilde{\lambda}$.

5. Application

5.1 Description of Taizhou Bridge over the Yangtze River

To verify the proposed approach, an experimental verification task is conducted for Taizhou Bridge. Taizhou Bridge, built in 2012, is a three-tower suspension bridge over the Yangtze River in China. As shown in Fig. 3, it has two consecutive main spans of 1080 m and side spans of 390 m. The total height of the central steel tower is 191.5 m and the side concrete towers are lower than the central tower by some 20 m. The foundation for the central tower, which is located in the centre of the river, is a caisson structure with cross-sectional dimensions of 58 m by 44 m. Foundations for the side towers are supported by 46 friction piles. Each of main cable consists of 184 prefabricated parallel wire strands, each of which consists of 91 high-strength galvanized 5.2

Fig. 3 View of the Taizhou Bridge

Table 2 The stiffness coefficients K_c, K_H, K_s for modes $n=1\sim5$

Mode	K_C* (kN/m)	K_H (kN/m)	K_S (kN/m)
$n=1$	2.10	6383.58	8936.91
$n=2$	16.79	25534.32	28274.35
$n=3$	85.01	57452.22	112061.88
$n=4$	268.67	102137.28	345292.89
$n=5$	655.94	159589.49	690264.67

*K_C, K_H, and K_S are related to the stiffness introduced by the elasticity of the main cable, the static tension H_w and the equivalent stiffness of the hangers and a girder.

mm-diameter steel wires with standard tensile strength of at least 1670 MPa. The Young's modulus, the inertia moment, the effective cross-sectional area and the equivalent specific weight of the main cable are 2×108 kPa, 0.0085 m^4, 0.3266 m^2 and 78.987 kN/m^3, respectively. The designed dead load horizontal component of main cable tension is . The sag-to-span ratio for the main cable is 1/9. Hangers are made of prefabricated parallel high strength 5 mm-diameter steel wires, again with a tensile strength of at least 1670 MPa. The typical spacing of hangers is 16 m and the tower centre-line is 20 m from the nearest hangers. The main girder is a streamlined, closed steel box girder cross-section, designed as a single box structure with three internal sections. The main girder is 3.5 m deep and 39.1 m width.

5.2 Influence of measured frequency deviations

Natural frequencies of the main cable obtained from dynamic test are necessary to estimate the tension force. Accounting for both the ambient noise and uncertainty of output-only characteristic frequencies identification, the influence of errors in characteristic frequencies could not be ignored on estimation of main cable parameters.

Table 3 Anti-symmetric characteristic frequencies for modes $n=1\sim5$

Mode	$n=1$	$n=2$	$n=3$	$n=4$	$n=5$
ω_{2n} * (rad/s)	0.987	1.988	3.489	5.669	7.814

*ω_{2n} is the anti-symmetric characteristic frequency.

Table 4 Estimation results of parameters of the main cable with frequency deviations

Frequency	*H_w (10^5 kN)			E_cI_c (10^6 kN·m^2)			m (10^1 ton/m)		
	Designed value	Estimated value	Error (%)	Designed value	Estimated value	Error (%)	Designed value	Estimated value	Error (%)
95% ω_{2n-1}	1.748	1.75	0.114	1.7	1.628	-4.24	2.5798	2.861	9.83
105% ω_{2n-1}	1.748	1.75	0.114	1.7	1.564	-8	2.5798	2.343	-9.18

*H_w is the horizontal tension of the main cable, E_cI_c is the flexural stiffness of the main cable and m is the combined mass of main cable and girder per unit length along the main cable.

According to Eqs. (18)-(20), the stiffness coefficients K_C, K_H, K_S for modes $n=1\sim5$ are presented in Table 2.

Then the anti-symmetric characteristic frequencies ω_{2n} could be obtained from Eq. (21), and the results of ω_{2n} for modes $n=1\sim5$ are shown in Table 3.

To investigate the error of the estimation due to characteristic frequency deviations, the first three anti-symmetric characteristic frequencies with ±5% deviation were used to estimate the main cable parameters H_w, E_cI_c, and m.

Firstly, the anti-symmetric characteristic frequencies with -5% deviations from the values in Table 3 were used to calculate the main cable parameters. From Eq. (36), the vector $\tilde{Z}$ was obtained as

$$\tilde{Z} = \begin{bmatrix} -8936.91 & -28274.35 & -112061.88 \end{bmatrix}$$

From Eq. (37), the matrix $\tilde{X}$ was obtained as

$$\tilde{X} = \begin{bmatrix} 0.0730 & 0.01826 & -0.4392 \\ 1.1686 & 0.07303 & -1.7839 \\ 5.9158 & 0.1643 & -5.4937 \end{bmatrix}$$

Substituting $\tilde{X}$ and $\tilde{Z}$ into Eq. (39), the vector $\tilde{\lambda}$ was obtained as

$$\tilde{\lambda} = \begin{bmatrix} 13.76 & 1.75\times10^5 & 3.09\times10^4 \end{bmatrix}$$

Then the anti-symmetric characteristic frequencies with 5% deviation from the values in Table 2 were used, and the vector $\tilde{\lambda}$ was obtained in a similar way

$$\tilde{\lambda} = \begin{bmatrix} 13.22 & 1.75\times10^5 & 2.53\times10^4 \end{bmatrix}$$

In Table 4, according to the frequencies with ±5% deviation the estimated results of H_w, E_cI_c and m were compared with the designed values. It can be observed that m is more sensitive to main cable frequencies than H_w and E_cI_c.
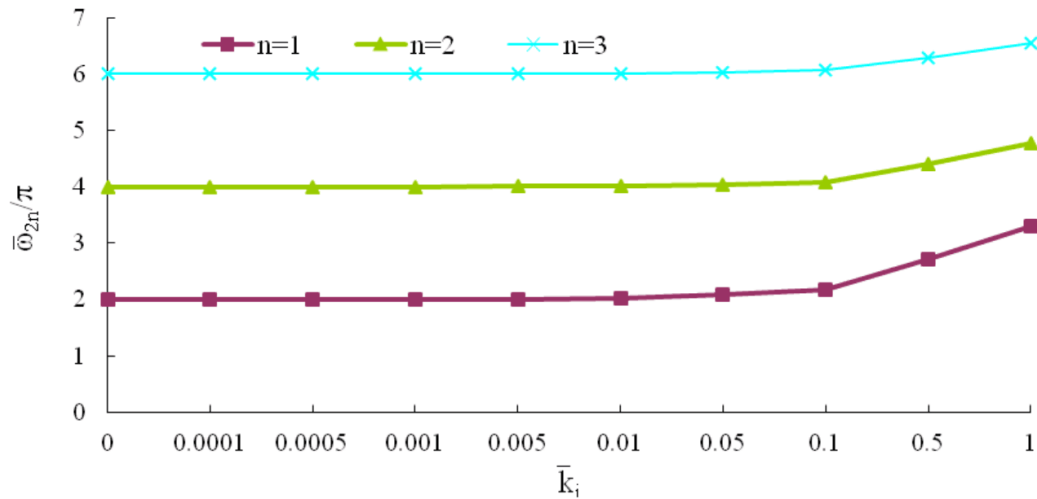
Fig. 4 Effects of $\bar{k}_i$ on the natural frequencies of the first three anti-symmetric modes

5.3 Influence of the stiffness of the girder and hangers

To study the influence of the stiffness of the girder and hangers on the natural frequencies of the main cable of Taizhou Bridge, Eq. (27) was used to calculate the first three anti-symmetric frequencies for designed value of μ_c^2, and for several values of $\bar{k}_i$ ranging from 0 to 1. As shown in Fig. 4, the low value of $\bar{k}_i$ (< 0.1) has a negligible effect on the first three anti-symmetric frequencies, but the effect becomes strong for higher value of $\bar{k}_i$ (> 0.1). The first three anti-symmetric frequencies increased 52.17%, 17% and 8.05%, respectively, as $\bar{k}_i$ increased from 0.1 to 1. It is indicated that the effect of $\bar{k}_i$ (>0.1) is progressively stronger on the lower modes.

If the effect of the stiffness of the girder and hangers on the vibration of the main cable of Taizhou Bridge was ignored ($\bar{k}_i = 0$), the first three anti-symmetric frequencies decreased 31.38%, 31.89% and 41.76%, respectively. The stiffness of the girder and hangers is found to have a significant influence on the anti-symmetric frequencies of the main cable of Taizhou Bridge.

5.4 Analytical modal analysis

To perform the analytical modal analysis of Taizhou Bridge, a three-dimensional finite element model (FEM) was established according to the design drawings using commercial software packages ANSYS 13.

The steel girders, concrete and steel towers are modeled by three-dimensional elastic beam elements (BEAM4). The middle tower is considered to be fixed at its base, while the platforms of the side towers are considered to be restrained with translational and rotational springs. The main cables and hangers are modeled by 3-D tension-only truss elements (LINK 10) since they are primarily designed to sustain tension forces. The main cables are divided into 386 truss elements and each hanger unit is modeled by a single element. The main span cables are considered as horizontal sagged cables fixed at the tower saddles and moving together with the towers, and the
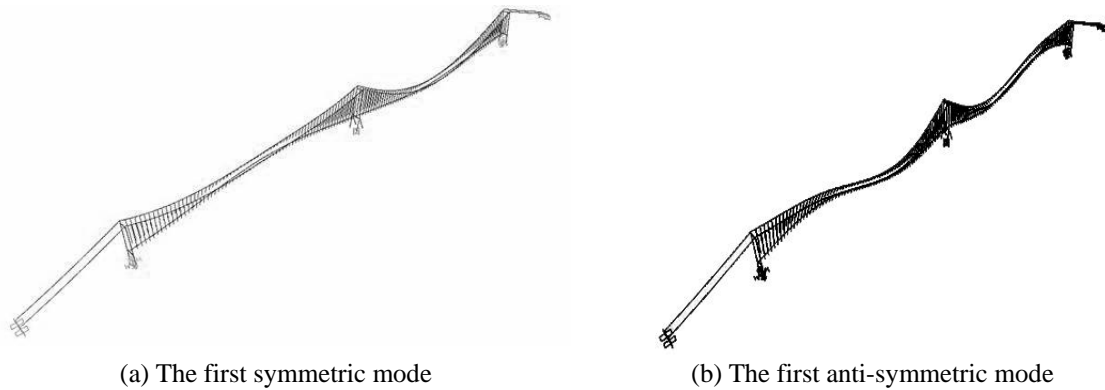
(a) The first symmetric mode   (b) The first anti-symmetric mode

Fig. 5 Vertical modes of Taizhou Bridge

Table 5 Summary of vertical modes of Taizhou Bridge

Mode	Frequency (Hz)			Nature of mode shape
	FEM	Eq.(21)	Error (%)	
1	0.1288	-	-	1st Vertical (Sym) *
2	0.1503	0.167	11.10%	2nd Vertical (Asym)
3	0.2332	-	-	3rd Vertical (Sym)
4	0.3279	0.313	4.54%	4th Vertical (Asym)
5	0.4521	-	-	5th Vertical (Sym)
6	0.4840	0.556	8.96%	6th Vertical (Asym)

*1st Vertical (Sym): The first type of mode is cables and deck in main span moving symmetrically.

side span cables are considered as inclined sagged cables with the top ends fixed at the tower saddles and the lower ends fixed at the main anchorage. The geometric nonlinearity is taken into account in the FEM due to the cable tension. The static equilibrium profiles of the main cables are calculated based on the static horizontal tensions and the unit weight of both cable and steel girder given in the design drawings. Rigid arms are accordingly assigned to the beam elements modeling the members at the joints.

The first vertical mode of the bridge is almost symmetric in the main span at a natural frequency of 0.1288 Hz, and the second vertical mode is anti-symmetric in the main span at a natural frequency of 0.1503 Hz, as shown in Fig. 5. Due to the suspenders, the motion of the main cables is always in phase with the motion of deck. The first five natural frequencies related to vertical vibration of bridge are listed in Table 5. Moreover, Table 5 gives a comparison between the anti-symmetric characteristic frequencies obtained from Eq. (21) and analytical natural frequencies. Results from the proposed formulae are found to be in good agreement with the numerical values.

5.5 Experiments

Final closure of the Taizhou Bridge was completed in September 2011, and then ambient vibrations of a main cable for Taizhou direction were measured with six accelerometers LC0115.

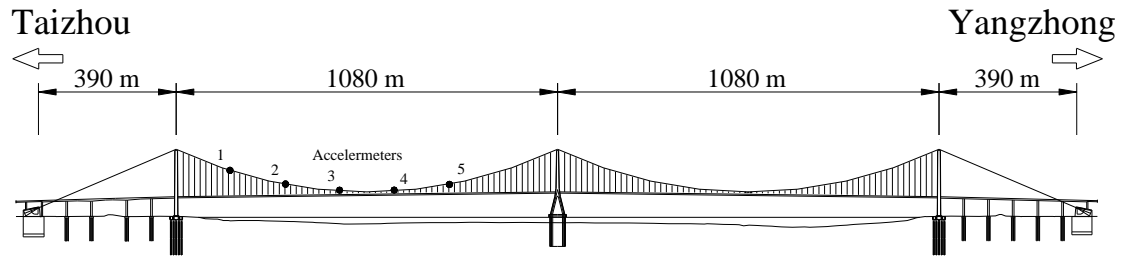Taizhou   Yangzhong

Fig. 6 Layout of accelerometers measuring vertical vibration

Fig. 7 Accelerometers mounted on the main cable

Among these accelerometers, five were used to measure the vertical vibration (Fig. 6), and one was used to measure the lateral vibration of the main cable (Fig. 7).

For frequency identification, only responses from accelerometers are utilized. These accelerometers have a range of frequency from 0.1 Hz to 1500 Hz. The acceleration time responses of the main cable were obtained with the sampling rate 0.2 s for 10 min and the data-sampling rate was 5 Hz. A rectangular window was applied to the time signals to minimize leakage. The vertical acceleration time histories are plotted in Fig. 8. Frequencies associated with peaks in the power spectral density function (PSD) of each recorded motion provided estimates of natural frequencies. The spectra of vertical accelerations obtained from five different locations on the main cable are shown in Fig. 9 and a typical cross-power spectrum between two response measurements (location 3 and location 4) is shown in Fig. 10. Hence, the first five actual frequencies of the main cable can be determined.
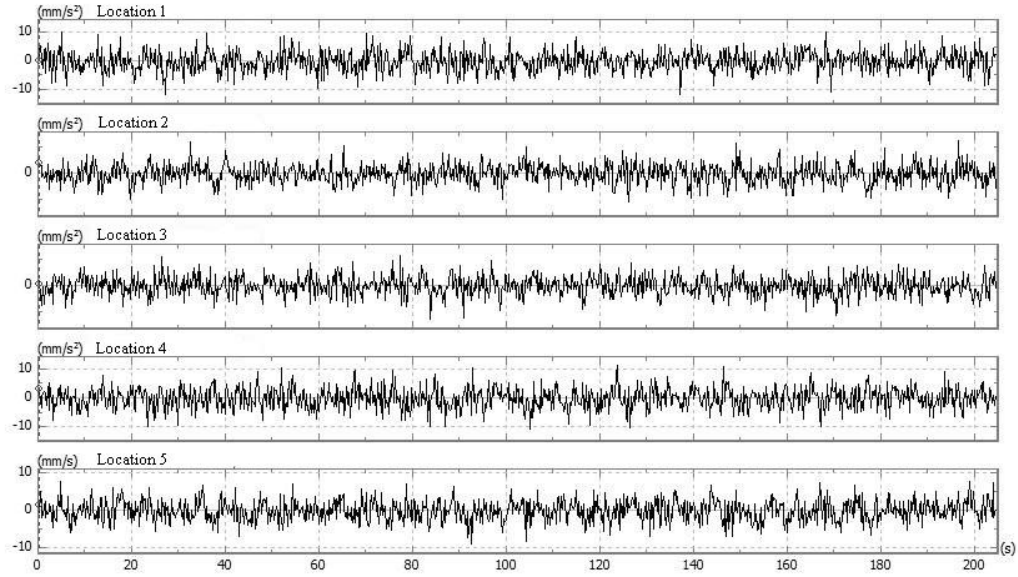
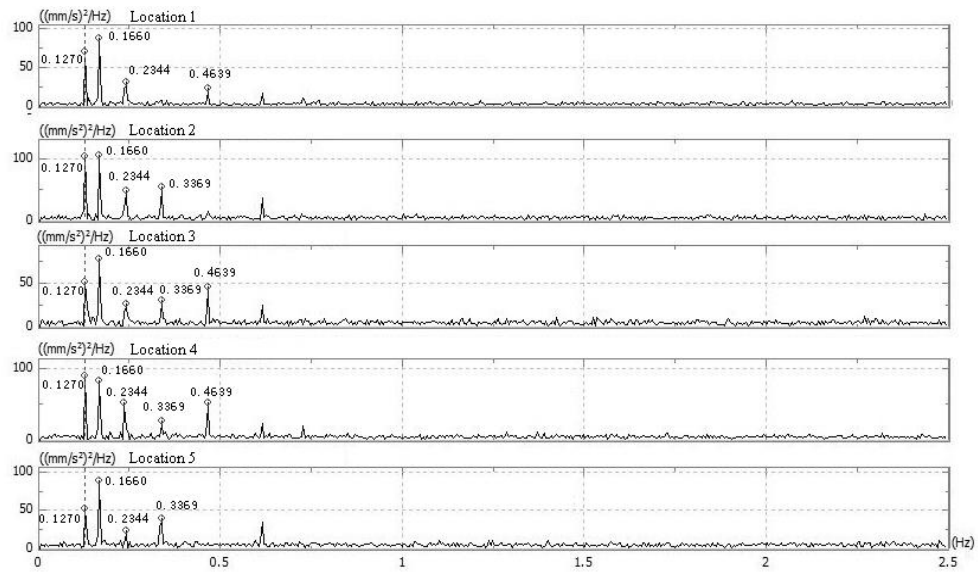Fig. 8 Vertical acceleration time histories recorded at different locations of the main cable

Fig. 9 PSDs of vertical accelerations measured on different locations of the main cable

The first three measured anti-symmetric frequencies (0.166, 0.337, and 0.612 Hz) were used to estimate the main cable parameters H_w, $E_c I_c$, and m.

From Eq. (37), the matrix $\tilde{X}$ was

$$\tilde{X} = \begin{bmatrix} 0.073 & 0.01826 & -0.5434 \\ 1.1686 & 0.07303 & -2.2395 \\ 5.9158 & 0.1643 & -7.3857 \end{bmatrix}$$
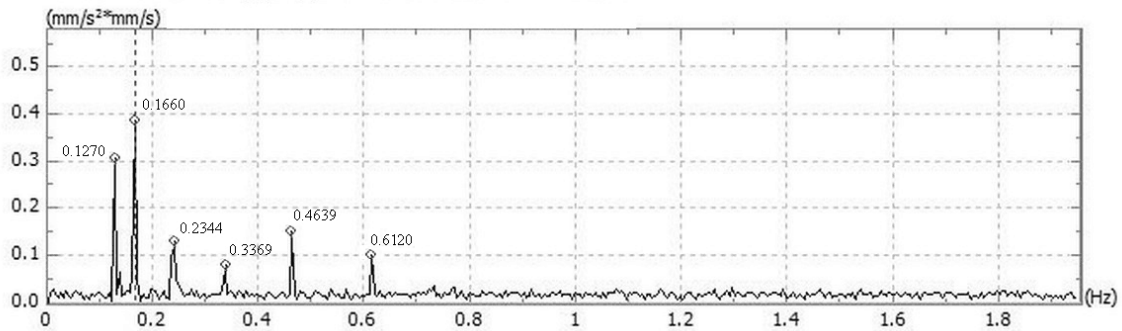
Fig. 10 Cross-power spectrum between response measurements of location 3 and location 4

Table 6 Comparison of estimation results from measured frequencies and designed values

H_w* (10^5 kN)			$E_c I_c$ (10^6 kNm^2)			m (10^1 ton/m)		
Designed value	Estimated value	Error (%)	Designed value	Estimated value	Error (%)	Designed value	Estimated value	Error (%)
1.748	1.734	-0.801	1.7	1.614	-5.06	2.5798	2.3801	-8.125

* H_w is the horizontal tension of the main cable, $E_c I_c$ is the flexural stiffness of the main cable and m is the combined mass of main cable and girder per unit length along the main cable.

From Eq. (41), the vector $\tilde{\lambda}$ was

$$\tilde{\lambda} = \begin{bmatrix} 13.64 & 1.7335 \times 10^5 & 2.5704 * 10^4 \end{bmatrix}$$

Therefore, parameters H_w, $E_c I_c$ and m are determined by $\tilde{\lambda}$. The estimated results are compared with designed values in Table 6. It can be observed that the estimated H_w and $E_c I_c$ agree well with the designed values. For the case of the estimated m, a relatively large variation is observed, compared to that of the estimated H_w and $E_c I_c$. This may be due to the fact that the extracted errors of frequencies have a relatively great effect on the estimation of m.

6. Conclusions

This study presents a simple and effective approach to estimate the main cable tension force from the measured frequencies. The main cable is considered as a uniform, elastic and flexural beam hinged at both towers and elastic supported by the girder and hangers along its entire length. When the hangers are located in the nodes of the $2n$ th mode, the influence of hangers on vibration of the main cable can be disregarded. The differential equation of the main cable is solved in the case of free motion by deriving anti-symmetric eigen frequencies and mode shapes in closed form, thus the sag does not generate the additional cable tension force in case of an anti-symmetric vibration mode. The anti-symmetric characteristic equation can be transformed into a least squares problem that can be solved efficiently to determine the main cable tension force.

Numerical study of the main cable of the Taizhou Bridge was carried out to examine the effects of deviations of the measured frequencies on the precision of estimation. It is shown that the

sensitivity of the combined mass of main cable and girder per unit length along the main cable is relatively larger than that of the horizontal tension and effective flexural stiffness of main cable. Moreover, ignoring the effect of the stiffness of the girder and hangers on the vibration of the main cable of Taizhou Bridge results in the decreases of 31.38%, 31.89% and 41.76% in the first three anti-symmetric frequencies, respectively. Finally, the field ambient experiments on the main cable of the Taizhou Bridge were conducted to obtain the natural frequencies before opening of the bridge to traffic. Comparison of the horizontal tension force of the main cable from estimated results and designed values shows a good agreement.

Acknowledgements

References

Yim, J.S., Wang, M.L., Shin, S.W., Yun, C.B., Jung, H.J., Kim, J.T. and Eem, S.H. (2013), "Field application of elasto-magnetic stress sensors for monitoring of cable tension force in cable-stayed bridges", *Smart Struct. Syst.*, **12**(3-4), 465-482.

Casas, J.R. (1994), "A combined method for measuring cable forces: The Cable-Stayed Alamillo Bridge, Spain", *Struct. Eng. Int.*, **4**(4), 235-240.

Fang, Z. and Wang, J.Q. (2012), "Practical formula for cable tension estimation by vibration meyhod", *J. Bridge Eng.*, ASCE, **17**(1), 161-164.

Ricciardi, G. and Saitta, F. (2008), "A continuous vibration analysis model for cables with sag and bending stiffness", *Eng. Struct.*, **30**(5), 1459-1472.

Nam, H. and Nghia, N.T. (2011), "Estimation of cable tension using measured natural frequencies", *Procedia Eng.*, **14**, 1510-1517.

Zui, H., Shinke, T. and Namita Y.H.(1996), "Practical formulas for estimation of the cable tension by vibration method", *J. Struct. Eng.*, ASCE, **124**(10), 651-656.

Yen, W.H.P., Mehrabi, A.B. and Tabatabai, H. (1997), "Evaluation of stay cable tension using a non-destructive vibration technique", *Proceedings of the 15th Structures Congress*, ASCE, New York, USA, April.

Mehrabi, A.B. and Tabatabai, H. (1998), "Unified finite difference formulation for free vibration of cables", *J. Struct. Eng.*, ASCE, **124**(11), 1313-1322.

Dan, D., Chen, Y. and Yan, X. (2014), "Determination of cable force based on the corrected numerical solution of cable vibration frequency equations", *Struct. Eng. Mech.*, **50**(1), 37-52.

Kim, B.H., Park, T., Shin, H. and Yoon, T.Y. (2007), "A comparative study of the tension estimation methods for cable supported bridges", *Steel Struct.*, **7**(1), 77-84.

Kim, M.Y., Kwon, S.D. and Kim, N.I. (2000), "Analytical and numerical study on free vertical vibration of shear-flexible suspension bridges", *J. Sound Vib.*, **238**(1), 65-84.

McKenna, P.J. and Walter, W. (1987), "Nonlinear oscillations in a suspension bridge", *Arch. Ration. Mech. An.*, **98** (2), 167-177.

Lazer, A.C. and McKenna, P.J. (1990), "Large-amplitude periodic oscillations in suspension bridges: some new connections with nonlinear analysis", *SIAM Rev.*, **32**(4), 537-578.

Glover, J., Lazer, A.C. and McKenna, P.J. (1989), "Existence and stability of large-scale nonlinear oscillations in suspension bridges", *Z. Angew. Math. Phys.*, **40**(2), 172-200.

Holubova-Tajcova, G. (1999), "Mathematical modeling of suspension bridges", *Math. Comput. Simulat.*,

50(1-4),183-197.

McKenna, P.J. and Moore, K.S. (2002), "The global structure of periodic solutions to a suspension bridge mechanical model", *IMA J. Appl. Math.*, **67**(5), 459-478.

Humphreys, L.D. and McKenna, P.J. (2005), "When a mechanical system goes nonlinear: Unexpected responses to low-periodic shaking", *Math. Assoc. Am.*, **112**(10), 861-875.

Turmo, J. and Luco, J.E. (2010), "Effect of hanger flexibility on dynamic response of suspension bridges", *J. Eng. Mech.*, ASCE, **136**(12), 1444-1459.

Konstantakopoulos, T.G. and Michaltsos, G.T. (2010), "A mathematical model for a combined cable system of bridges", *Eng. Struct.*, **32**(9), 2717-2728.

Luco, J.E. and Turmo, J. (2010), "Linear vertical vibrations of suspension bridges: a review of continuum models and some new results", *Soil Dyn Earthq. Eng.*, **30**(9), 769-781.

Ni, Y.Q., Ko, J.M. and Zheng, G. (2002), "Dynamic analysis of large-diameter sagged cables taking into account flexural rigidity", *J. Sound Vib.*, **257**(2), 301-319.

Kim, B.H. and Park, T. (2007), "Estimation of cable tension using the frequency-based system identification method", *J. Sound Vib.*, **304**(3-5), 660-676.

Wang, H., Li, A.Q. and Li, J. (2010), "Progressive finite element model calibration of a long-span suspension bridge based on ambient vibration and static measurements", *Eng. Struct.*, **32**(9), 2546-2556.

Brownjohn, J.M.W., Xia, P.Q., Hao, H. and Xia, Y. (2001), "Civil structure condition assessment by FE model updating: methodology and case studies", *Finite Elem. Anal. Des.*, **37**(10), 761-775.

Schlune, H., Plos, M. and Gylltoft, K. (2009), "Improved bridge evaluation through finite element model updating using static and dynamic measurements", *Eng. Struct.*, **31**(7), 1477-1485.

Liao, W.Y., Ni, Y.Q. and Zheng, G. (2012), "Tension force and structural parameter identification of bridge cables", *Adv. Struct. Eng.*, **15**(6), 983-995.

Timoshenko, S.P. and Young, D.H. (1965), *Theory of Structures*, McGraw-Hill Book Company, New York, USA.

Steinman, D.B. (1953), *A Practical Treatise on Suspension Bridges*, Wiley, New York, USA.

Irvine, H.M. and Caughey, T.K. (1974), "The linear theory of free vibration of a suspended cable", *Proceedings of the Royal Society of London, Serious A*, London, UK, December.

CC